Journal of Physics: Conference Series **712** (2016) 012026 doi:10.1088/1742-6596/712/1/012026

XAFS at the new materials science beamline 10 at the DELTA storage ring

D Lützenkirchen-Hecht*, R Wagner, R Frahm
Bergische Universität Wuppertal, Gaußstr. 20, 42097 Wuppertal, Germany

*E-mail: dirklh@uni-wuppertal.de

Abstract. The layout and the characteristics of the hard X-ray beamline BL 10 at the superconducting asymmetric wiggler at the 1.5 GeV Dortmund Electron Accelerator DELTA are described. Equipped with a stable and robust Si(111) channel-cut monochromator, this beamline is suited for XAFS studies in the spectral range from about 4 keV to ca. 16 keV photon energy. We will illustrate the performance of the beamline, and present EXAFS data obtained from several reference compounds. XANES data measured for dilute sample systems as well as surface sensitive grazing incidence EXAFS obtained from thin film samples will also be discussed.

1. Introduction

The DELTA synchrotron radiation facility (1.5 GeV electron energy, injection currents of ~120 mA, lifetime 10-15 h) is equipped with several beamlines providing radiation from the UV-visible spectral range to hard X-rays [1]. In order to increase X-ray related research activities, and to meet the user needs for high energy photons especially for spectroscopic studies, a new hard X-ray beamline was installed, making use of the intense radiation emitted by a superconducting asymmetric wiggler (SAW) with a critical energy of about 7.9 keV. The broad radiation fan of this insertion device covers about ± 25 mrad horizontal beam divergence, so that the installation of a third beamline (BL10) at this insertion device in parallel to the two existing ones [2, 3] is feasible, however with some restrictions in terms of the space available for the newly installed instrumentation. In this contribution, we will describe the optical layout and the performance of this new beamline, including some experimental data from user experiments.

2. Beamline overview

Due to the angular offset of 15 mrad between BL 10 and the adjacent beamline 9, there is only a limited space available for the added instrumentation of BL 10, especially in the front-end and the optics hutches. Therefore, the installation of X-ray mirrors for focusing, suppression of higher harmonics and for a reduction of the heat load on the monochromator was not possible, and BL10 has a very simple X-ray optical layout. It consists of a fixed, water-cooled absorber mask ca. 12 m from the center of the wiggler source that delivers a radiation fan of 3 mrad x 0.7 mrad (horiz. x vert.) into the beamline, a tilt absorber in a distance of 23.8 m, which is used for the definition of the vertical beam size impinging on the compact, Si(111) channel-cut monochromator that is installed in the experimental hutch 30 m from the source [4]. As proved by finite element calculations, the thermal distortions and slope errors of the first monochromator crystal surface induced by the heat load of the

wiggler of about 1.59 W mrad^{-2} mA^{-1} (corresponding to about 0.2 W mm^{-2} for 100 mA of stored electron current) are significantly smaller compared to the Darwin width of the employed Si(111) crystal [4]. Furthermore, changes of the heat load on the monochromator due to the decrease of the electron current in the storage ring have no measurable influence on the monochromator resolution, and observed shifts of the energy scale are smaller than 0.1 eV. Downstream the monochromator, two slit systems finally define the size of the monochromatic beam on the sample. Two different setups are permanently installed in the experimental hutch: (a) a table for standard transmission and fluorescence mode EXAFS experiments using gas-filled ionization chambers and different photodiodes with related detector electronics as detectors, and (b) a 6-axis Kappa-diffractometer, that can be employed for all kinds of diffraction studies, and grazing incidence EXAFS experiments [4, 5]. A typical photon flux at the position of the sample amounts to 5*10^{9} photons s^{-1} mm^{-2} at 8 keV and 100 mA of stored current.

The use of a channel-cut monochromator and the absence of mirrors make harmonic rejection a critical issue for the present beamline. However, due to the critical energy of the wiggler source of only 7.9 keV, the flux decreases substantially for photon energies above 10 keV. Furthermore, if the filling gases of the ionization chambers are chosen properly, the sensitivities for the higher order harmonics are further reduced, so that a harmonic suppression of at least 5*10^{-3} or better can be achieved [4]. XAFS experiments of different reference materials have shown that the harmonic suppression achieved at BL 10 appears sufficient for high quality XANES and EXAFS studies.

Due to the simple layout of the beamline, the different detector systems available and the flexibility of the equipment for employing e.g. cryostats (down to 77 K), high temperature reaction cells (300 K – ca. 1500 K) or vacuum chambers (p < 10^{-8} mbar), it is ideally suited for educational purposes, and several projects with students have been performed in the first few months of operation.

3. XAFS experiments

3.1. Transmission mode EXAFS

In the commissioning phase of BL 10, several different metal foils in the energy range from the Ti K-edge (4966 eV) to the Au L_1-edge (14353 eV) have been examined by transmission mode EXAFS at room temperature for reference purposes. In general, the obtained data quality is excellent with respect to the reproduction of sharp absorption features close to the edges as well as to the low noise of the k^3-weighted $\chi(k)$ data as can be seen in figure 1, where a representative example of a Ta-metal foil measured at room temperature within about 35 minutes is shown. The extracted k^3-weighted $\chi(k)$ data are almost noise-free up to wavenumbers of 18 Å^{-1}, i.e. more than 1200 eV above the edge. It should be noted that the measured k-range is only limited by the onset of the Ta L_2-absorption edge at 11136 eV. The experimental results show that the energy resolution of the channel-cut monochromator is close to the values expected from the values for the natural width of the absorption edges of interest, (see ref. [4]) and thus high resolution XANES and EXAFS experiments in the energy range between ca. 4 keV and 16 keV are feasible at BL 10.

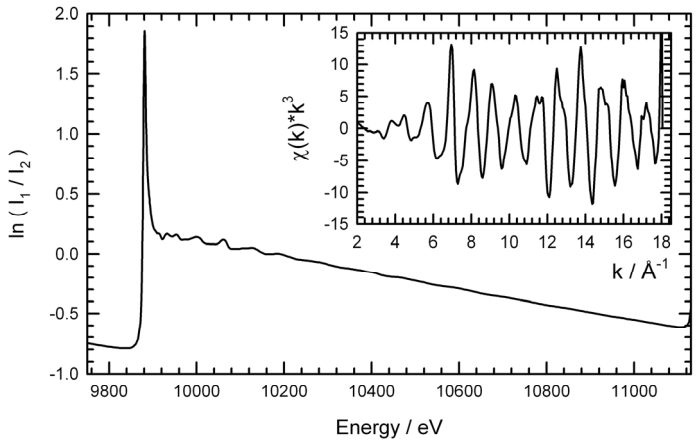

Figure 1. L_3-edge X-ray absorption spectrum of a Ta metal foil measured in transmission at room temperature. In the inset, the k^3-weighted fine structure oscillations $\chi(k) * k^3$ are depicted. The onset of the Ta L_2-edge can be seen in the absorption spectrum at about 11130 eV, and at ca. 18 Å^{-1} in the k^3-weighted $\chi(k) * k^3$ data, respectively.

3.2. Fluorescence mode XANES

Besides transmission mode experiments, fluorescence detection is feasible at BL10 using large area PIPS (passivated implanted planar silicon) detectors or an energy dispersive Peltier-cooled Si drift-diode with digital pulse processing electronics. As an example, we have recently investigated doped barium aluminate ($BaAl_2O_4$) samples. These materials are of particular interest because of their luminescence properties when they are doped with rare earth or transition metal cations [6, 7]. However, in the case of Cr-doping, the measurement of the K-edge of the dopant is extremely difficult, because the L_1-edge of the Ba host has an identical energy of 5989 eV, making transmission mode experiments impossible. As can be seen in figure 2(a), also the fluorescence emissions from the Cr dopant and the $BaAl_2O_4$ host lattice are heavily overlapping, with intense Ba L-lines at about 4460, 4830, 5160 and 5530 eV, and relatively weak Cr K-emissions at 5410 and 5950 eV. However, with a careful setting of the region in the fluorescence spectrum used for the calculation of an EXAFS spectrum, the overlap can be minimized, and absorption data of reasonable data quality can be achieved (see figure 2(b)). The comparison of the measured data with those of reference compounds ($BaCrO_4$, Cr_2O_3) shows that the Cr incorporated in the doped samples seems to be in a 6+ state, and the coordination is mainly tetrahedral, as can be anticipated from the intense pre-edge peak at 5993 eV and the edge position at about 6009 eV, which is further supported by a linear combination XANES fit of the edge region (not shown).

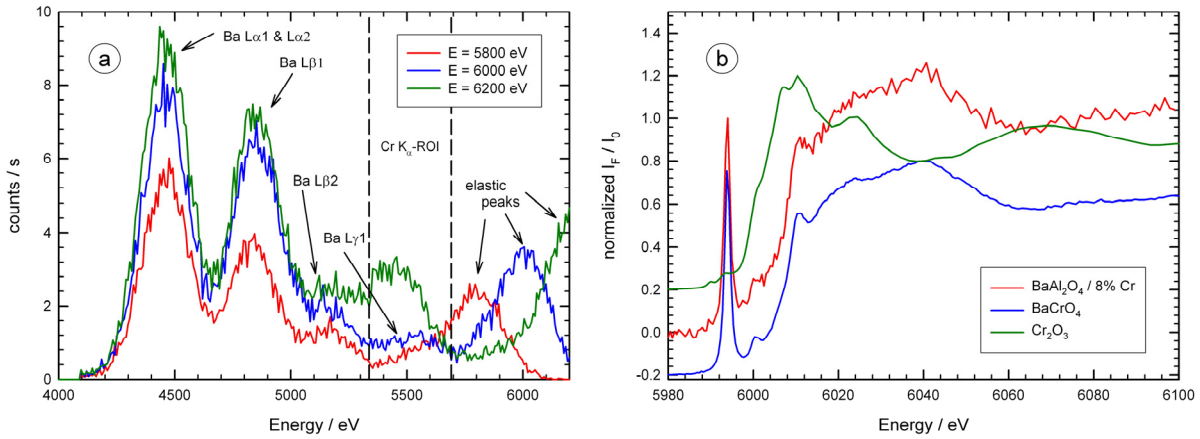

Figure 2. (a) X-ray fluorescence spectra from a $BaAl_2O_4$ sample doped with 8 at.% Cr for different excitation energies in the vicinity of the Cr K-edge / Ba L_1-edge. Emissions between ca. 5350 eV and 5700 eV are mainly caused by the Cr-fluorescence. (b) Cr K-edge near edge spectrum of $BaAl_2O_4$ sample doped with 8 at.% Cr in comparison to K-edge spectra of barium chromate ($BaCrO_4$) and Cr_2O_3.

3.3. Grazing incidence XAFS

Grazing incidence X-ray absorption spectroscopy is an excellent method to study the near surface structure of thin films, surfaces, adsorbates etc. (e.g. refs. [5, 8-11]) and it has also been used in the past for the investigation of intermetallic layers [8]. Here we have *in-situ* explored the formation of NiAl induced by a heat treatment of Al-Ni-bilayers in vacuum using Ni K-edge XAFS. The samples were prepared by thermal evaporation of Al and Ni on float glass substrates under high-vacuum. According to X-ray reflectivity measurements, the thickness of the Al and Ni layers amount to about 80 nm and 72 nm, respectively. For temperatures below 200°C, the measured XAFS data closely resembles the spectrum of metallic Ni metal, while NiAl formation starts at about 210°C. In figure 3, in-situ measured XAFS spectra for different incidence angles Θ are displayed for a substrate temperature of 230°C, and spectra of a NiAl reference sample and Ni metal are shown for comparison. As can be seen in figure 3, the XAFS data from the bilayer sample closely resemble that of the NiAl reference for incidence angles below the critical angle of total reflection of Ni, while they are

dominated by XAFS fine structure of Ni metal for larger incidence angles $\Theta > 0.35°$. The present results suggest that a thin NiAl-film has formed at the interface between the metallic Al- and Ni-sublayers. From a fit of the experimental data (not shown), the thickness of this layer can be estimated to about 10 nm. Experiments at more elevated temperatures show that the NiAl film thickness is not increasing further, and it should also be noted that no evidence for other Ni-Al compounds such as $NiAl_2$, Ni_2Al_3 etc. could be obtained in the present study.

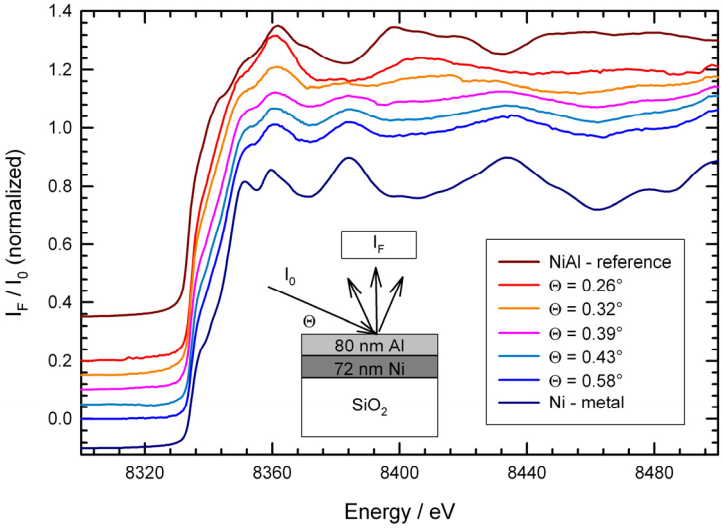

Figure 3. Grazing incidence XAFS at the Ni K-edge measured *in-situ* during the annealing of a Al/Ni-bilayer on a glass substrate at T = 230°C. X-ray absorption spectra were measured in fluorescence mode using a large area PIPS diode for different incidence angles Θ as indicated in the inset. For comparison, the spectrum of a NiAl intermetallic compound and a Ni-metal reference are also shown.

4. Conclusions

In conclusion, the instrumentation of BL 10 at the DELTA storage ring provides the conditions for a wide range of XAFS investigations. The robust and stable Si(111) channel-cut monochromator covers the energy range from ca. 4 – 16 keV, allowing XAFS experiments at the K- or L-edges of most of the technologically important elements. Besides transmission and fluorescence detection modes, grazing incidence EXAFS experiments are feasible making use of the multi-purpose diffractometer, also for studies in different non-ambient environments (vacuum, gas and liquid phase, cryogenic and high temperature). The results presented here demonstrate that high quality EXAFS data can be achieved at beamline 10 in various different sample environments, making BL 10 thus an attractive instrument for EXAFS studies with hard X-rays.

References

[1] Tolan M, Weis T, Wille K and Westphal C 2003 *Synchrotron Rad News* **16** 9
[2] Paulus M, Fendt R, Sternemann C, Gutt C, Hövel H, Volmer M, Tolan M and Wille K 2005 *J. Synchrotron Rad.* **12** 246
[3] Lützenkirchen-Hecht D, Wagner R, Haake U, Watenphul A and Frahm R 2009 *J. Synchrotron Rad.* **16** 264
[4] Lützenkirchen-Hecht D, Wagner R, Szillat S, Hüsecken AK, Istomin K, Pietsch U and Frahm R 2014 *J. Synchrotron Rad.* **21** 819
[5] Lützenkirchen-Hecht D, Wulff D, Wagner R, Frahm R, Holländer U and Maier HJ 2014 *J. Mater. Sci.* **49** 5454
[6] Fukuda K, Iwata T and Orito T 2005 *J. Solid State Chem.* **178** 3662
[7] Lin Y, Zhang Z, Tang Z, Zhang J, Zheng Z and Lu X 2001 *Mater. Chem. Phys.* **70** 156
[8] Heald SM, Chen H and Tranquada JM 1988 *Phys. Rev. B* **38** 1016
[9] Borthen P and Strehblow H-H 1995 *J. Phys.: Condens. Matter* **7** 3779
[10] Jiang DT and Crozier ED 1998 *Can. J. Phys.* **76** 621
[11] d'Acapito F, Emelianov I, Relini A, Cavatorta P, Gliozzi A, Minicozzi V, Morante S, Solari PL and Rolandi R 2002 *Langmuir* **18** 5277